

Structure H Hydrate Phase Equilibria of Paraffins, Naphthenes, and Olefins with Methane

Ajay P. Mehta and E. Dendy Sloan, Jr.*

Center for Research on Hydrates, Chemical Engineering and Petroleum-Refining Department, Colorado School of Mines, Golden, Colorado 80401

Initial phase equilibrium data are reported for 10 methane + liquid hydrocarbon systems forming structure H hydrates in the pressure range of 1-6 MPa. Four-phase equilibrium conditions were measured for each system, with paraffinic, naphthenic, and olefinic liquid hydrocarbons filling the large cage of structure H, and methane stabilizing the two smaller cages present in the hydrate. Many of these liquid hydrocarbons constitute a small fraction of crude oils and condensates, and the high stability and relative ease of formation of structure H suggest a possible impact of these hydrates upon hydrocarbon facilities.

Introduction

Gas hydrates are inclusion compounds, in which a hydrogen-bonded network of water molecules forms clusters around dissolved gas molecules, resulting in a three-dimensional crystal lattice. Because solid hydrate crystals form large aggregates which can plug flow channels and cause hydrate blockages in deep-sea pipelines, they are a major concern in the oil industry. Hydrate formation is generally favored at temperatures around the ice point at high pressures.

Hydrates are known to occur in two different crystal forms, commonly known as Structure I (sI) and structure II (sII). Many simple molecules like methane, propane, carbon dioxide, and hydrogen sulfide form either one of these hydrate structures. Hydrates of types sI and sII have been studied extensively, and a recent review by Sloan (1) provides a comprehensive summary of these structures. Structure H (sH) hydrate was discovered in 1987 by Ripmeester et al. (2) who showed that sH hydrate could form from large molecules like methylcyclohexane which are indigenous to petroleum. Unlike sI and sII hydrates, sH was shown to be a double hydrate, requiring the presence of small help gas molecules like Xe or H₂S along with a large hydrocarbon molecule to be stable. They found that sH was composed of three different types of cages—two small cages of comparable size, which could accommodate small molecules like Xe, and a large nonspherical cage, which could accommodate molecules in the size range of 7.5-8.6 Å. Single crystal data on sH hydrate are not currently known, but X-ray and powder diffraction data obtained by Ripmeester et al. (2) show that it is isostructural with the hexagonal clathrasil dodecasil-1H reported by Gerke and Gies (3).

Ripmeester and Ratcliffe (4) identified 24 large molecules which could form sH in the presence of Xe and H₂S; Table 1 lists the various substituted alkanes, alkenes, alkynes, cycloalkanes, and cycloalkenes identified as sH formers. Some of the listed sH formers like 2-methylbutane (isopentane) and methylcyclopentane were assumed by Katz et al. (5) to be non-hydrate formers. In addition, guests with several other functional groups like ketones and ether can also form sH. The first phase equilibrium data on sH hydrates were reported by Lederhos et al. (6) for methane + adamantane. Adamantane is one of the chief constituents of diamondoids which are known to exist *in situ* with methane and free water in deep-water reservoirs, including Mobile Bay in the Gulf of Mexico. Recently Cullick et al.

Table 1. Structure H Hydrate Formers Identified by Ripmeester and Ratcliffe (4)

alkane	alkene/alkyne	cycloalkane/alkene
2-methylbutane	2,3-dimethyl-1-butene	methylcyclopentane
2,2-dimethylbutane	2,3-dimethyl-2-butene	methylcyclohexane
2,3-dimethylbutane	3,3-dimethyl-1-butene	<i>cis</i> -1,2-dimethylcyclohexane
2,2,3-trimethylbutane	3,3-dimethyl-1-butyne	cyclooctane
2,2-dimethylpentane		adamantane
3,3-dimethylpentane		cycloheptene
hexamethylethane		<i>cis</i> -cyclooctene
		bicyclo[2.2.2]oct-2-ene

(7) have shown that small amounts of hydrocarbon diamondoid compounds can precipitate as solids at surface flowline conditions. The phase equilibrium data of sH for methane + adamantane suggest that sH hydrates may coexist with solid diamondoid deposits.

Mehta and Sloan (8) measured the sH phase equilibrium conditions for three liquid hydrocarbons: 2-methylbutane, 2,2-dimethylbutane, and methylcyclohexane, each with methane as the help gas. Becke et al. (9) also independently reported sH data at high pressures for methane + methylcyclohexane. Recently, Thomas and Behar (10) have reported sH equilibrium data for thirteen systems of methane and an intermediate hydrocarbon molecule in the pressure range of 3-12 MPa, including four new sH forming large molecules, cycloheptane, ethylcyclohexane, ethylcyclopentane, and 1,1-dimethylcyclohexane, which had not been previously identified by Ripmeester and Ratcliffe (4).

In this work, we report new phase equilibrium measurements on 10 sH forming binary mixtures in the pressure range of 1-6 MPa. Our results complement the high-pressure data of Thomas and Behar (10) for the paraffinic and naphthenic components with the exception of the methane + 2,2-dimethylpentane system. Initial sH data are also presented for four systems containing a large olefin guest molecule and methane. Since many of these sH formers constitute a small fraction of crude oils and condensates, these phase equilibrium conditions for sH suggest a possible impact upon both natural and artificial aspects of hydrocarbon reservoirs where such molecules can be found in association with molecules like H₂S and CH₄ at low temperatures and high pressures.

Experimental Apparatus and Procedure

All the large liquid hydrocarbons were purchased from either Aldrich Chemical Co. or Fluka Chemical Co. and had

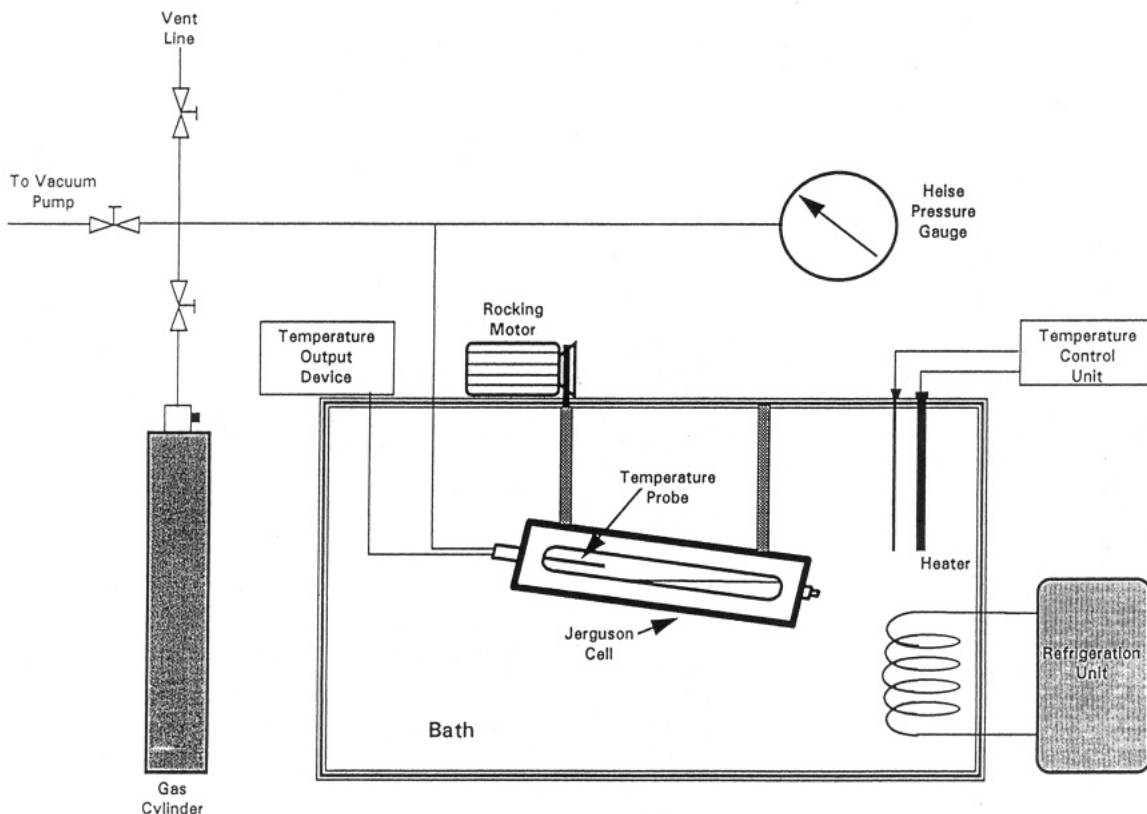


Figure 1. Experimental apparatus.

a minimum purity of 98+%. Methane gas with a purity of 99.99% was obtained from General Air Products. The chemicals were used as received without any further purification. Deionized water was used in all experiments.

The experimental apparatus is shown in Figure 1 and consists of a Jerguson sight glass cell which was rocked about its axis. The cell was immersed in a refrigerated constant-temperature bath regulated by a Bayley precision controller accurate to within ± 0.1 K. The bath was equipped with a Plexiglas window to allow visual monitoring of hydrate formation or dissociation. The temperature was sensed by a platinum resistance thermometer accurate to within 1% in the 273–300 K range, and the cell pressure was measured by a Heise pressure gauge accurate to within $\pm 0.1\%$ of the full-scale reading.

In order to avoid difficult composition measurements, the experimental procedure took advantage of the Gibbs phase rule. The univariance of the system was established since the three components liquid water, liquid hydrocarbon, and methane combined to form four phases at equilibrium: water-rich liquid L_W , hydrocarbon-rich liquid L_{HC} , vapor V , and sH hydrate. Thus, setting the temperature at which these four phases coexist uniquely determined all the other intensive parameters, such as pressure, gas composition, and hydrate composition.

Initially 60–75 cm³ of deionized water and a 100% stoichiometric excess of the liquid hydrocarbon were inserted into the cell. Since water and the liquid hydrocarbon are virtually insoluble in each other, two distinct liquids could be seen visually. The air was evacuated by pumping on the system and then charged with methane above the sI equilibrium pressure. After sI hydrates were formed, the pressure was reduced to a point below the sI hydrate equilibrium to dissociate the sI hydrates, leaving behind residual hydrogen bonds and some labile clusters in the aqueous phase and thereby promoting the formation of sH hydrate. After the system stabilized, a subsequent drop

in the pressure would indicate consumption of gas due to sH formation, and the system pressure was assumed to be above the sH equilibrium point. On the other hand, an increase in the pressure would indicate sH dissociation via the release of gas, and the system pressure was assumed to be below the sH equilibrium. In this manner the system pressure was monitored constantly, and by successive charging and venting cycles, the sH equilibrium pressure was located within an accuracy of ± 30 kPa.

With most of the liquid hydrocarbons it was necessary to pressurize the system above the sI equilibrium to initiate sH formation. However, in the presence of a few sH formers like 2,3-dimethylbutane, 2,2,3-trimethylbutane, and *cis*-cyclooctene, if the run was started at a pressure above the sI equilibrium, there was a catastrophic formation of hydrates. The pressure did not initially stabilize at the pure methane sI equilibrium as with the other systems but continued to drop until a dense plug of hydrates filled up the entire cell. So in subsequent runs, the system was initially charged to a pressure lower than the sI equilibrium, sharp drops in the pressure via sH formation were recorded, and the sH equilibrium could be located using the same procedure as explained above.

Results and Discussion

Table 2 contains the sH phase equilibrium results for systems with substituted methylbutanes and methylpentanes, Table 3 for systems with cycloalkanes and cycloalkenes, and Table 4 for systems with substituted methylbutenes. Figure 2 shows all the available sH data of methane + substituted methylbutanes plotted with the data of sI methane hydrates measured by Deaton and Frost (11). It can be seen that each of the sH four-phase equilibrium lines lie below the sI three-phase equilibrium line for pure methane. There is also good agreement between our low-pressure results and the high-pressure values of Thomas and Behar (10).

Table 2. sH Hydrate Phase Equilibrium Data of Methane + Substituted Methylbutanes/Pentanes

component	T/K	P/MPa
2,3-dimethylbutane	275.87	2.078
	277.37	2.482
	279.20	3.088
	280.84	3.795
2,2,3-trimethylbutane	275.65	1.475
	277.40	1.840
	279.53	2.247
	280.90	2.702
2,2-dimethylpentane	275.87	3.287
	277.40	3.819
	279.20	4.556
	280.34	5.832
3,3-dimethylpentane	274.81	1.734
	276.98	2.264
	279.17	3.009
	281.31	3.930

Table 3. sH Hydrate Phase Equilibrium Data of Methane + Cycloalkanes/Alkenes

component	T/K	P/MPa
methylcyclopentane	276.51	2.199
	277.78	2.578
	279.54	3.195
	280.78	3.812
<i>cis</i> -1,2-dimethylcyclohexane	275.76	1.871
	277.45	2.237
	279.37	2.816
	281.01	3.433
cycloheptene	275.09	2.106
	277.71	2.671
	279.21	3.051
	280.98	3.809
<i>cis</i> -cyclooctene	276.90	2.082
	278.48	2.562
	279.95	3.009
	281.28	3.561

Table 4. sH Hydrate Phase Equilibrium Data of Methane + Substituted Methylbutenes

component	T/K	P/MPa
2,3-dimethyl-1-butene	275.67	2.530
	277.78	3.275
	279.53	4.088
	280.78	4.805
3,3-dimethyl-1-butene	276.20	2.016
	277.65	2.423
	279.20	2.933
	281.42	3.871

Figure 3 shows the results for two sH forming methylpentanes, and there is good agreement between our work and the data of Thomas and Behar (10) for the system of methane + 3,3-dimethylpentane. There is a large discrepancy between our low-pressure values of methane + 2,2-dimethylpentane and that of Thomas and Behar (10). In our experiments it was difficult to distinguish between the sH and sI equilibrium since the sH equilibrium pressures were lying just slightly below those of sI; nevertheless, the difference was well beyond the bounds of experimental inaccuracy. However, the methane + 2,2-dimethylpentane value of Thomas and Behar (10) measured at three temperatures between 286 and 290 K shows their sH equilibrium line to lie far below that of sI. This discrepancy between the two data sets could be due to different purities of the chemicals used or to some other unknowns in either experiment. It also suggests, however, that there may be a structural transition occurring between sI and sH hydrates at intermediate temperatures between 280 and 286 K; investigations in this temperature range are currently being carried out in our laboratory.

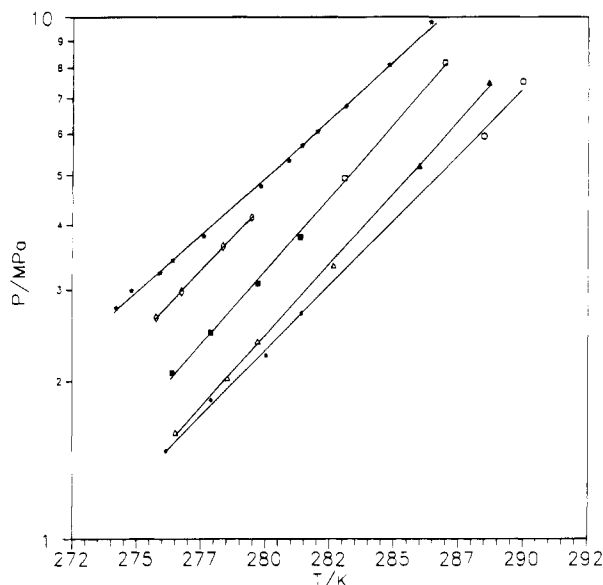


Figure 2. sH equilibria for methane + substituted methylbutanes compared with sI methane equilibria: (★) sI methane, ref 11; (◇) sH 2-methylbutane + methane, ref 8; (■) sH 2,3-dimethylbutane + methane, this work; (□) sH 2,3-dimethylbutane + methane, ref 10; (△) sH 2,2-dimethylbutane + methane, ref 9; (▲) 2,2-dimethylbutane + methane, ref 10; (●) sH 2,2,3-trimethylbutane + methane, this work; (○) sH 2,2,3-trimethylbutane + methane, ref 10.

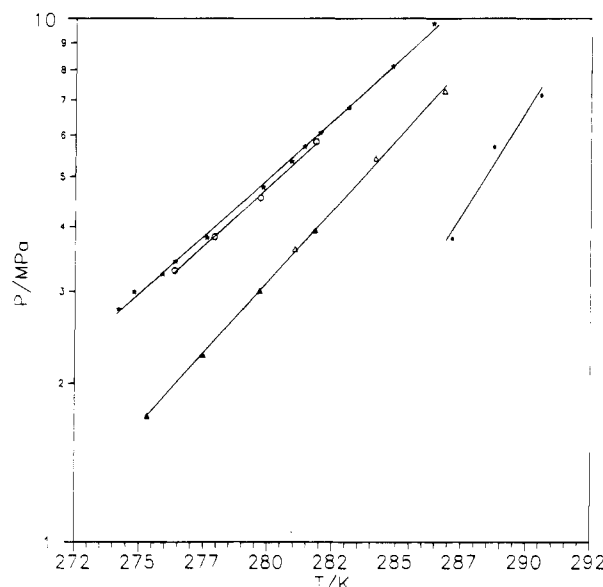


Figure 3. sH equilibria for methane + substituted methylpentanes compared with sI methane equilibria: (★) sI methane, ref 11; (○) sH 2,2-dimethylpentane + methane, this work; (◇) sH 2,2-dimethylpentane + methane, ref 10; (▲) sH 3,3-dimethylpentane + methane, this work; (△) sH 3,3-dimethylpentane + methane, ref 10.

Figure 4 shows good agreement between our data and those of Thomas and Behar (10) for three methane + methylcycloalkane systems. The slopes of these sH equilibrium lines are remarkably similar, suggesting a constant enthalpy of dissociation for these systems. Figure 5 shows our results for the systems of methane + methylbutenes and methane + cycloalkenes. No phase equilibrium data for these sH forming alkenes or cycloalkenes have been reported elsewhere.

An interesting feature of sH hydrates is the difference in the equilibrium pressures between systems with molecules having similar size. For example, Figure 2 shows

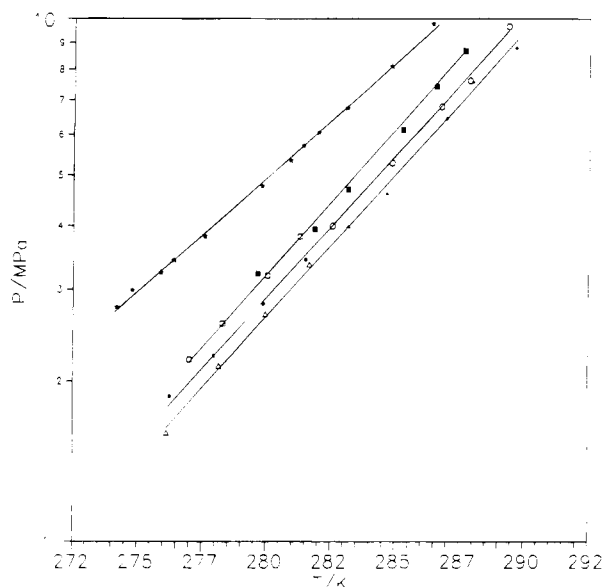


Figure 4. sH equilibria for methane + methylcycloalkanes compared with sI methane equilibria: (★) sI methane, ref 11; (□) sH methylcyclopentane + methane, this work; (■) sH methylcyclopentane + methane, ref 10; (●) sH *cis*-1,2-dimethylcyclohexane, this work; (○) sH *cis*-1,2-dimethylcyclohexane + methane, ref 10; (Δ) sH methylcyclohexane + methane, ref 8; (▲) sH methylcyclohexane + methane, ref 10.

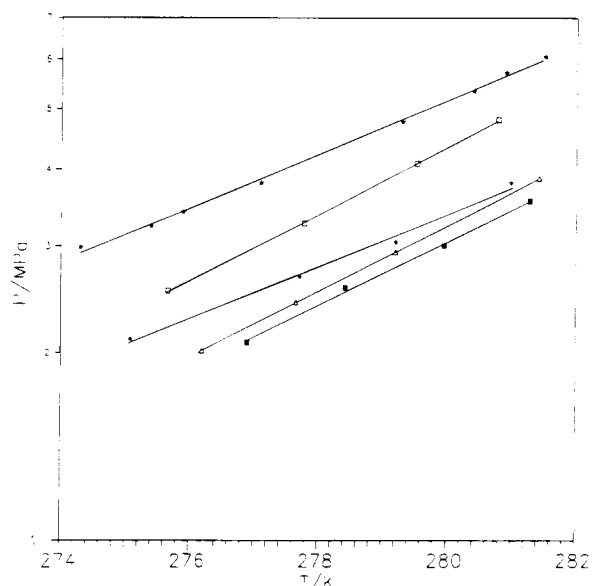


Figure 5. sH equilibria for methane + alkenes/cycloalkenes: (★) sI methane, ref 11; (□) sH 2,3-dimethyl-1-butene + methane, this work; (●) cycloheptene + methane, this work; (Δ) 3,3-dimethyl-1-butene + methane, this work; (■) *cis*-cyclooctene, this work.

that there is a considerable difference between the equilibrium pressures of methane + 2,2-dimethylbutane and methane + 2,3-dimethylbutane. Similar stability differences are also exhibited between the systems of methane + 2,2-dimethylpentane and methane + 3,3-dimethylpentane shown in Figure 3. Moreover, 2,3-dimethylpentane

and 2,4-dimethylpentane do not form sH at all. Thus, unlike sI and sII hydrates where all molecules of the correct size form a hydrate, sH molecules of similar sizes need not all be hydrate formers. It has been pointed out by Ripmeester and Ratcliffe (4) that the shape of the molecule and efficient space filling of the large nonspherical cage of sH to maximize the van der Waals contact between the guest molecule and the water framework are important considerations for sH formation. Ripmeester and Ratcliffe (4) as well as Thomas and Behar (10) have listed several paraffins and naphthenes which have the right size but still do not participate in sH formation. A correlation between some molecular property of these hydrocarbons and their ability to form sH would greatly improve the statistical thermodynamic model of Mehta and Sloan (12) for sH hydrates.

Conclusions

Initial phase equilibrium results for 10 sH forming systems have been presented. Our low-pressure data are found to be consistent with the high-pressure data of Thomas and Behar for most systems. The temperature and pressure conditions at which sH forms are consistent with those of hydrocarbon processing and transportation. The relative ease of sH formation suggests that it may occur naturally, perhaps in association with other hydrate structures in regions of oil and gas fields rich in these hydrocarbons. The partitioning of crude oil and certain sH forming molecules may have implications in petroleum geochemistry. The wide range of molecules which can stabilize sH suggests that sH hydrate may represent the largest family of hydrate formers.

Acknowledgment

The authors would like to acknowledge the efforts of undergraduate student Jim McCulloch for his assistance in obtaining some of the sH data presented in this paper.

Literature Cited

- (1) Sloan, E. D., Jr. *Clathrate Hydrates of Natural Gas*; Marcel Dekker: New York, 1990.
- (2) Ripmeester, J. A.; Tse, J. S.; Ratcliffe, C. I.; Powell, B. M. *Nature* **1987**, *325* (6100), 135.
- (3) Gerke, H.; Gies, H. Z. *Kristallogr.* **1984**, *166*, 11.
- (4) Ripmeester, J. A.; Ratcliffe, C. I. *J. Phys. Chem.* **1990**, *94* (25), 8773.
- (5) Katz, D. L., Ed. *Handbook of Natural Gas Engineering*; McGraw-Hill: New York, 1959; p 209.
- (6) Lederhos, J. P.; Mehta, A. P.; Nyberg, G. B.; Warn, K. J.; Sloan, E. D. *AIChE J.* **1992**, *38* (7), 1045.
- (7) Cullick, A. S.; Magouirk, J. L.; Ng, H. J. Presented at the 73rd GPA Convention, New Orleans, March 7–9, 1994.
- (8) Mehta, A. P.; Sloan, E. D. *J. Chem. Eng. Data* **1993**, *38*, 580.
- (9) Becke, P.; Kessel, D.; Rahiman, I. *SPE 25032* **1992**, 159.
- (10) Thomas M.; Behar, E. Presented at the 73rd GPA Convention, New Orleans, March 7–9, 1994.
- (11) Frost, W. M.; Frost, E. M. *U.S. Bur. Mines Monogr.* **1946**, 8.
- (12) Mehta, A. P.; Sloan, E. D. *AIChE J.* **1994**, *40* (2), 312.

Received for review April 18, 1994. Accepted May 30, 1994.* We also gratefully acknowledge the National Science Foundation for supporting this work under Grant CTS-9309595.

* Abstract published in *Advance ACS Abstracts*, August 15, 1994.